

Do Anionic Titanium Dioxide Nano-Clusters Reach Bulk Band Gap? A Density Functional Theory Study

ZHENG-WANG QU,¹ HUI ZHU²

¹Humboldt Universität zu Berlin, Institut für Physik, AG Photobiophysik, D-12489 Berlin, Germany

²Freie Universität Berlin, Institute for Mathematics, D-14195 Berlin, Germany

Received 1 July 2009; Revised 9 November 2009; Accepted 25 November 2009

DOI 10.1002/jcc.21488

Published online in Wiley InterScience (www.interscience.wiley.com).

Abstract: The electronic properties of both neutral and anionic $(\text{TiO}_2)_n$ ($n = 1\text{--}10$) clusters are investigated by extensive density functional theory calculations. The predicted electron detachment energies and excitation gaps of anionic clusters agree well with the original experimental anion photoelectron spectra (APES). It is shown that the old way to analyze APES tends to overestimate vertical excitation gaps (VGA) of large anionic clusters, due to the nature of multiple electronic origins for the higher APES bands. Moreover, the VGA of anionic TiO_2 clusters are evidently smaller than those of neutral clusters, which may also be the case for other metal oxide clusters with high electron affinity.

© 2010 Wiley Periodicals, Inc. J Comput Chem 00: 000–000, 2010

Key words: titanium dioxide (TiO_2); cluster; DFT; excitation gap; photoelectron spectrum; electron affinity

Introduction

Nano-structured metal oxide materials can exhibit unique structural, electronic, and chemical properties due to their limited size and high density of surface corner or edge sites, and have been widely used for many important applications such as catalysis and photo-catalysis, quantum computing, ultra high-density magnetic data storage, and more recently spintronics.^{1–4} The size-dependent properties such as optical band gap and surface structures of nano-particles are crucial for these important applications and thus have attracted a lot of experimental and theoretical interests. In particular, as a cheap and chemically and biologically inert semiconductor with a wide band gap (3.0 eV for rutile and 3.2 eV for anatase phase), titanium dioxide (TiO_2) has become one of the most technologically important oxide materials and a prototype transition metal oxide system for surface science.^{5,6} Normally, TiO_2 may exist in nature mainly as the most stable rutile crystal, while the anatase phase becomes more stable than the rutile phase when the particle diameters of TiO_2 are smaller than about 14 nm.⁷ If the particles become really small, they may of course have structures that cannot be derived from the bulk structure.

As a traditional and powerful technique, anion photoelectron spectroscopy (APES) has been widely used to explore electronic structures such as electron affinities of a wide range of molecules and clusters.⁸ Recently, there are extensive interests to extend this technique to explore the size-dependent excitation gaps of transition metal oxide clusters such as $(\text{TiO}_2)_n$ ($n = 1\text{--}$

10),^{9,10} $(\text{CrO}_3)_n$ ($n = 1\text{--}5$),¹¹ $(\text{V}_2\text{O}_5)_n$ ($n = 2\text{--}4$),¹² and $(\text{WO}_3)_n$.¹³ Surprisingly, it is commonly found that the APES-derived excitation gaps (so-called band gaps)^{9–13} increase rapidly to reach the bulk band gaps. However, it is well-known that the optical excitation gaps of a semiconductor material to the nanometer scale may change as the function of particle size due to quantum confinement effects^{2–7} that should cause a blue-shift (increase) of band gap with respect to that of bulk. A clear blue-shift of excitation gaps has been observed for metal oxide nanoparticles such as Fe_2O_3 , ZnO , and CdO .^{2–5} There is a long debate on if such quantum confinement effects exist for TiO_2 nano-particles.^{4,5,14,15} According to our recent B3LYP/LANL2DZ calculations,^{16,17} it seems that the excitation gaps of neutral TiO_2 clusters tends to decrease with increasing cluster sizes. In this work, we will present reliable B3LYP/6-31+G(d) calculations to resolve this contradiction.

Computational Methods

Before presenting our density functional theory (DFT) results, it is helpful to make clear several useful energetic quantities concerning both anionic and neutral TiO_2 nano-particles, as shown

Additional Supporting Information may be found in the online version of this article.

Correspondence to: Z.-W. Qu; e-mail: zheng@physik.hu-berlin.de

schematically in Figure 1. Normally, a neutral $(\text{TiO}_2)_n$ cluster has a singlet electronic ground state, with the lowest triplet and singlet excited states being very close in energy within 0.1 eV.^{16,17} After one electron attachment, the anionic cluster has a doublet ground state with the extra electron localized on a Ti atom. To be more specific, two kinds of processes need to be distinguished: they are adiabatic or vertical depending on if the final cluster geometry is fully relaxed or fixed with respect to the starting geometry, and will be indicated by prefixes “A” and “V” in this work, respectively. The processes relevant to this work can be the electron detachments of anionic clusters (or the electron attachment of neutral clusters as the reverse process) and the electronic excitations of neutral clusters. To distinguish with the electron detachment/attachment processes between neutral and anionic clusters and to be consistent with literature,^{9–13} the term of “gap” will be used for the lowest excitation energies from the neutral electronic singlet ground state only. As usual, for a neutral $(\text{TiO}_2)_n$ cluster in the singlet ground state, the electron affinity (EA) is defined as the energy released after electron attachment leading to the anionic doublet state, while the excitation gaps can be defined as the excitation energies to the lowest singlet or triplet excited states. As the spin-allowed singlet-singlet transitions are readily observable from experimental optical spectra, the vertical excitation gaps (VGN) to the lowest singlet excited state are calculated in this work. In APES experiments, however, both singlet and triplet electronic states can be reached after electron detachment of anionic $(\text{TiO}_2)_n^-$ cluster due to the lack of spin restraint for such processes. For an anionic $(\text{TiO}_2)_n^-$ cluster in the doublet ground state, the first and second electron detachment energies (DE) are defined as the energy needed to remove one electron leading to the singlet ground state (so-called X band) and to the higher excited states (so-called A band)^{9,10} of neutral cluster, respectively. Although both the lowest singlet and triplet excited states will contribute to the broad A band, we use the slightly lower energy of the lowest triplet excited state for calculating the second DE value for direct comparison with experiment. Then, the excitation gap of an anionic cluster is taken as the difference between the second and the first DE values. The vertical EA will be abbreviated to VEA, and so on. By definition the adiabatic electron affinity (AEA) and adiabatic electron detachment energy (ADE) should take the same value. It is the vertical electron detachment energy (VDE), vertical excitation gap of anionic cluster (VDA), ADE (or AEA), and adiabatic excitation gaps (AGA) rather than VGN and VEA values that could be directly extracted from experimental APES spectra in favorable cases.

Experimentally, though the ADE, VDE, and AGA values for each mass-selected $(\text{TiO}_2)_n^-$ cluster¹⁰ could be estimated directly from the measured APES spectra, the detailed cluster structures are unfortunately unknown. In order to compare our DFT predicted energetics with the APES estimated data,¹⁰ we assume that only one or several lowest-lying isomers for each $(\text{TiO}_2)_n^-$ cluster can contribute predominantly to the observed APES spectra. Experimentally,¹⁰ the $(\text{TiO}_2)_n^-$ clusters were produced by laser vaporization of a pure Ti disk target in the presence of a He carrier gas seeded with 0.5% O₂ and mass-selected, with effort to control the cluster temperature and to choose colder clusters for photo-detachment. Under such “annealing” experi-

mental conditions, such assumption with contribution only from several lowest-lying isomers should be reasonable, as also supported by many successful theoretical simulations of APES spectra of other metal oxide anions.^{10–12,18,19}

Extensive DFT calculations are performed to explore the lowest-lying structures of both anionic and neutral $(\text{TiO}_2)_n$ ($n = 1–10$) clusters, using the hybrid B3LYP functional^{20–22} and the all-electron 6-31+G(d) basis set^{23,24} as implemented in the Gaussian 03 program.²⁵ The 6-31+G(d) basis set consists of 87 basis functions per TiO_2 unit including also polarization and diffuse functions on Ti and O atoms that is crucial for reliable description of electronic structures of the anionic and excited states. In addition to some previously suggested $(\text{TiO}_2)_n$ cluster structures,^{16,17,26,27} further efforts are made in this work to identify the global minima of large clusters with $n \geq 4$ that may have many low-lying isomers. The largest $(\text{TiO}_2)_{10}$ cluster with a diameter of about 1 nm can be taken as the benchmark to understand the size-dependent electronic properties of nanoparticles. Triplet neutral clusters are also optimized using unrestricted B3LYP to derive AGA with essentially the same accuracy of ground-state B3LYP. To provide reliable VGN, time-dependent DFT (TDDFT) calculations^{28–30} at the B3LYP/6-31+G(d) level are also performed for 10 lowest singlet and 10 lowest triplet excited states at both the neutral and the anionic minima of each $(\text{TiO}_2)_n$ cluster. Zero-point vibrational energy corrections are calculated by frequency analysis and included in the predicted ADE (or AEA) and AGA values. The experimental APES spectra could be simulated by using the DFT-derived ADE (AEA), VDE, VEA, and AGA values as well as the TDDFT-derived VGN and VGA values. The good performance of B3LYP functional has been well established by successful applications to various transition metal oxide clusters of CrO₃,¹¹ V₂O₅,^{12,18,21} WO₃,^{13,19} and TiO₂.^{16,17,26,27,32}

Results and Discussion

Figure 2 shows the B3LYP/6-31+G(d) optimized lowest-lying anionic $(\text{TiO}_2)_n^-$ ($n = 1–10$) structures, among which **5a**⁻, **7a**⁻, **8a**⁻, and **10a**⁻ are not found in previous studies but newly found in this work. (More detailed anionic, neutral singlet, and neutral triplet structures of up to three higher-lying isomers for each n -value are listed in Supporting Information Fig. S1.) Anionic structures not shown in Figure 2 are mostly at least 0.3 eV higher in energy, which thus should be irrelevant to the APES experiment under normal ambient conditions. Table 1 lists the B3LYP/6-31+G(d) predicted energetics (in eV) for up to three lowest-lying isomers of both anionic and neutral $(\text{TiO}_2)_n$ clusters. These energetic data include the total energies relative to the selected low-lying anionic relative energy of anionic cluster and neutral relative energy of neutral cluster (REA) and (REN); some of each cluster as zero reference, the ADE: adiabatic electron detachment energy, VDE: vertical electron detachment energy, AGA, and VGA: vertical excitation gap of anionic cluster values for anionic clusters, and the AEA: adiabatic electron affinity, VEA and VGN: vertical excitation gap of neutral cluster values for neutral clusters as defined above. Note that by definition the AEA and first ADE should take the same value, while

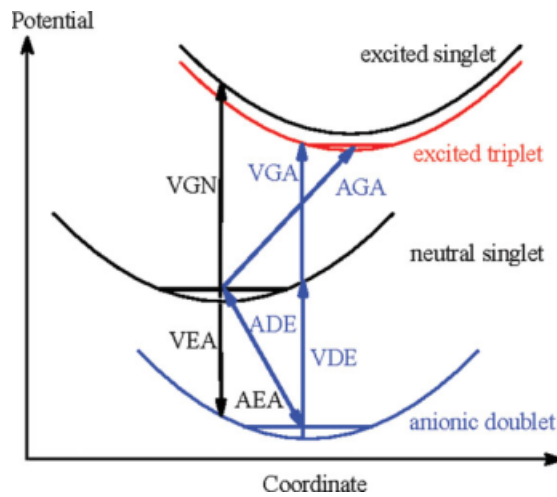


Figure 1. The schematic definition of various energetic quantities of anionic and neutral $(\text{TiO}_2)_n$ clusters. To distinguish from the processes involving electron detachment (or attachment), the term “gap” is used for the lowest excitation energies from the neutral electronic singlet ground state only. For anionic clusters, the ADE and VDE stand for the adiabatic and vertical electron detachment energies, the AGA and VGA for the adiabatic and vertical excitation gaps to the lowest triplet excited state, respectively. For neutral clusters, the VGN stands for the vertical excitation gap to the lowest singlet excited state, the AEA and VEA for the adiabatic and vertical electron affinities, respectively. By definition the AEA and first ADE should take the same value, while the AGA value is the same as the adiabatic excitation gap of the neutral cluster to the lowest triplet excited state.

the AGA of the neutral cluster to the lowest triplet excited state is the same as the AGA of the corresponding anionic cluster. The B3LYP/LANL2DZ predicted AEA values¹⁶ as well as some experimentally estimated ADE, VDE and AGA data¹⁰ are also included here for comparison. Note that the stability order of isomers of some neutral clusters could be reversed after electron attachment due to different electron affinities. For example, the isomer **4a** of neutral $(\text{TiO}_2)_4$ cluster is 0.260 and 0.379 eV more stable than the isomers **4b** and **4c**; however, after electron attachment the corresponding anionic isomer **4a**⁻ becomes 0.040 and 0.158 eV less stable than **4b**⁻ and **4c**⁻, respectively. These near-degenerate low-lying anionic isomers may contribute together to the observed broad electron detachment bands of $(\text{TiO}_2)_4$.^{9,10} However, in most cases as shown in Figure 2, the experimental APES spectra are expected to be dominated by only one lowest-lying anionic isomer of each cluster.

In the recent DFT study³² of bare and dye-sensitized TiO_2 clusters and nano-particles with sizes smaller than 2 nm, different structures were optimized from truncated anatase bulk crystal structure. For very small clusters with $n = 1, 2$, and 3, the resultant stable structures³² are the same as the predicted global minima in this work. However, for larger clusters the structures truncated directly from anatase bulk³² become higher-lying in energy. For example, the truncated structures³² with $n = 4, 6$, and 16 are also found in our previous B3LYP/LANL2DZ studies,^{16,17} but they are 0.6, 1.8, and 5.9 eV higher in energy than the corresponding (predicted) global minima,^{16,17} suggesting that small TiO_2 nano-clusters should assume some structures different from bulk anatase structure.

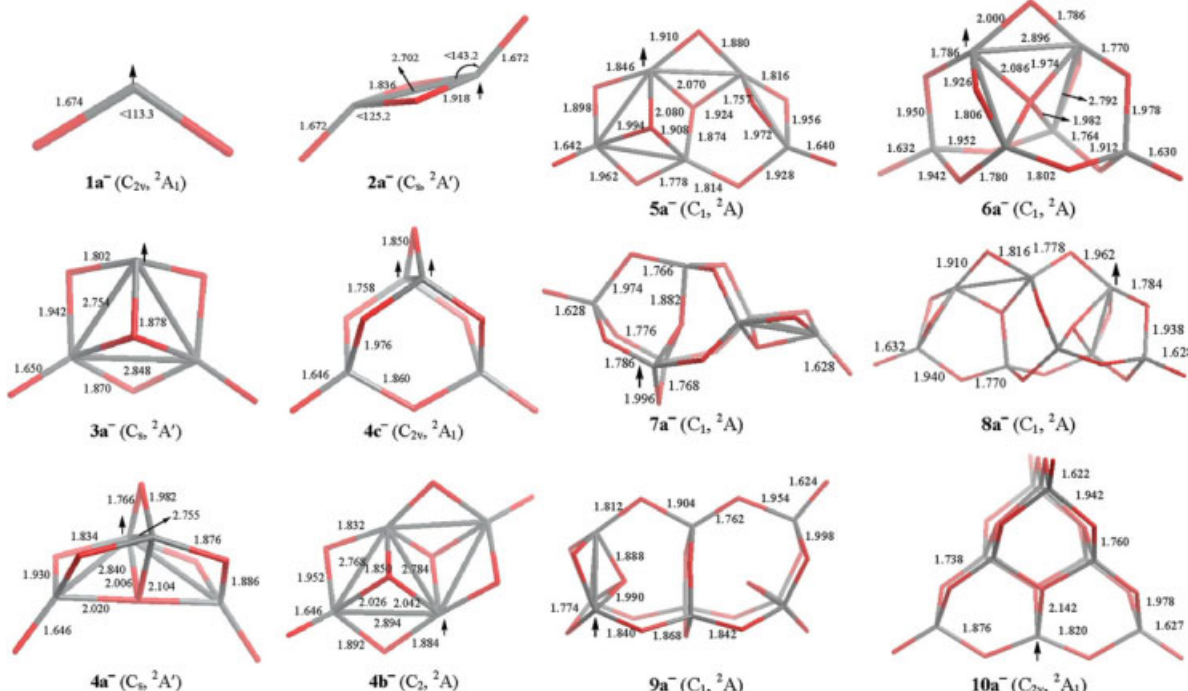


Figure 2. The B3LYP/6-31+G(d) optimized geometries of the lowest-lying anionic $(\text{TiO}_2)_n$ ($n = 1$ –10) clusters. Within each cluster the localized spin density is indicated by a vertical arrow. The Ti-atoms are shown in grey and O-atoms in red, with typical Ti—O bond lengths given in Å.

Table 1. The B3LYP/6-31+G(d) Predicted Energetics (in eV) for Both Anionic and Neutral $(\text{TiO}_2)_n$ Clusters with Cluster Size $n = 1\text{--}10$ and a Comparison with Experimentally (Ref. 9) Estimated Data.

Anion	Calc								Expt. ^a			
	REA	REN	ADE	AEA ^b	VDE	VEA	AGA	VGA	VGN	ADE	VDE	AGA
1a ⁻	0.000	0.000	1.688	1.69	1.730	1.630	1.981	2.557	2.638	1.59 (3)	1.59 (3)	2.22 (10)
2a ⁻	0.000	0.000	1.910	2.12	2.368	1.604	2.327	3.009	3.742	2.06 (5)	2.27 (5)	2.59 (10)
2b ⁻	0.420	0.696	2.186		2.440	1.929						
3a ⁻	0.000	0.000	3.071	3.32	3.496	2.663	1.853	1.953	3.002	2.78 (10)	3.15 (5)	2.26 (10)
3b ⁻	1.203	0.413	2.299		2.773	1.979						
4a ⁻	0.000	0.000	2.837	3.33	3.672	1.963	2.309	2.461	3.918	3.00 (15)	3.65 (5)	2.60 (15)
4b ⁻	-0.040	0.260	3.137		3.945	2.364	2.036	2.219	3.560			
4c ⁻	-0.158	0.379	3.374	3.44	4.043	2.860	1.391	1.268	2.441			
5a ⁻	0.000	0.000	3.168		4.197	2.471	2.153	2.048	3.926	3.15 (20)	4.13 (10)	2.85 (20)
5b ⁻	0.393	-0.013	2.763	3.24	3.689	2.027	2.879	2.459	3.831			
6a ⁻	0.000	0.000	3.242	3.68	4.049	2.605	2.261	2.407	3.967	3.20 (20)	4.00 (10)	3.00 (20)
6b ⁻	0.472	0.609	3.348		3.938	2.456						
6c ⁻	0.925	0.527	2.844		4.258	2.210						
7a ⁻	0.000	0.000	3.133		4.022	2.457	2.383	2.580	4.136	3.30 (25)	4.20 (15)	3.10 (25)
7b ⁻	0.354	0.421	3.200		4.184	2.532	2.338	2.259	3.923			
7c ⁻	0.404	0.720	3.449	3.92	4.332	2.711	1.978	2.137	3.616			
8a ⁻	0.000	0.243	3.453		4.316	2.749	2.359	2.124	4.142	3.5 (3)	4.70 (15)	3.1 (3)
8b ⁻	0.167	0.000	3.029		3.875	2.518	2.442	2.676	4.081			
8c ⁻	0.297	0.247	3.173		4.027	2.594	2.338	2.445	3.976			
9a ⁻	0.000	0.000	3.403	3.94	4.377	2.431	1.958	1.517	3.638	3.6 (3)	4.75 (15)	3.1 (3)
9b ⁻	0.373	0.358	3.388		4.466	2.692	2.210	1.994	3.757			
9c ⁻	0.430	0.861	3.834		5.085	3.558	2.104	2.013	3.472			
10a ⁻	0.000	0.249	4.047		5.015	3.447	2.278	2.278	3.812	3.6 (3)	4.80 (15)	3.1 (3)
10b ⁻	0.364	0.000	3.434		4.327	2.846	2.380	2.283	3.930			

The data include the total energies relative to the selected low-lying anionic (REA) and neutral (REN) isomer of each cluster as zero reference, the adiabatic (ADE) and vertical (VDE) electron detachment energies of anionic cluster, the adiabatic (AEA) and vertical (VEA) electron affinities of neutral cluster, the adiabatic (AGA) and vertical (VGA) excitation gaps of anionic cluster, and the vertical excitation gaps of neutral cluster (VGN).

^aThe experimentally estimated data taken from Ref. 9.

^bThe B3LYP/LANL2DZ predicted values taken from Ref. 15.

Some common structural features can be observed for the optimized lowest-lying anionic $(\text{TiO}_2)_n^-$ and neutral $(\text{TiO}_2)_n$ ($n = 1\text{--}10$) clusters. First, one terminal Ti=O bond ($\sim 1.6 \text{ \AA}$) in an anionic (or neutral) structure is elongated by about 0.2 \AA in the corresponding triplet structure due to a localized hole (electron vacancy) on the terminal O-atom. Second, the extra electron in each anionic (or excited electron in each triplet) structure is localized on a least-coordinated Ti-atom, around which the Ti—O bonds are elongated by more than 0.1 \AA . Third, the Ti—O bonds further away from the localized hole and excited (or extra) electron are alternately shortened and elongated to a lesser extent as compared with the corresponding singlet neutral structure. For example, within the anionic structure **3a**⁻ the extra electron is localized on a three-coordinated Ti-atom, with the surrounding Ti—O bonds being about 0.07 \AA longer than those within neutral structure **3a** (see Supporting Information Fig. S1). These structural features suggest that it is the Ti—O stretch vibration modes that are most likely excited upon electron detachment of an anionic cluster. Due to the additional effects of localized hole, a triplet $(\text{TiO}_2)_n$ cluster may show larger structural relaxation than the corresponding anionic cluster with the effects of only localized extra-electron, as shown

schematically in Figure 1. The electron detachment of an anionic $(\text{TiO}_2)_n^-$ cluster may lead to the singlet ground state (X band) or the higher triplet and singlet excited states (A band) of the corresponding neutral cluster. Thus, according to our frequency analysis, the excited vibration modes should mainly correspond to the stretch of terminal Ti=O around 1000 cm^{-1} (for small clusters with $n = 1$ and 2) and bridging Ti—O—Ti around 850 cm^{-1} for the X band, and to the stretch of terminal Ti—O around 650 cm^{-1} and bridging Ti—O—Ti around 850 cm^{-1} for the A band, respectively. Experimentally, only the X band of TiO_2^- is vibrationally resolved^{9,10}; the observed vibrational spacing of about 0.12 eV (970 cm^{-1}) is consistent with our theoretical analysis.

Figure 3 shows the simulated APES spectra of the lowest-lying $(\text{TiO}_2)_n^-$ anionic clusters along with a comparison with the available experimental spectra.¹⁰ The crucial energetic data such as ADE, VDE, and AGA for these and higher-lying anionic and neutral clusters are listed in Table 1, which may be used to simulate the APES spectra of other clusters. For each anionic cluster, the ADE and VDE values should be consistent with the onsets and the maxima of each electron detachment band, respectively. However, the experimental APES spectra are further complicated

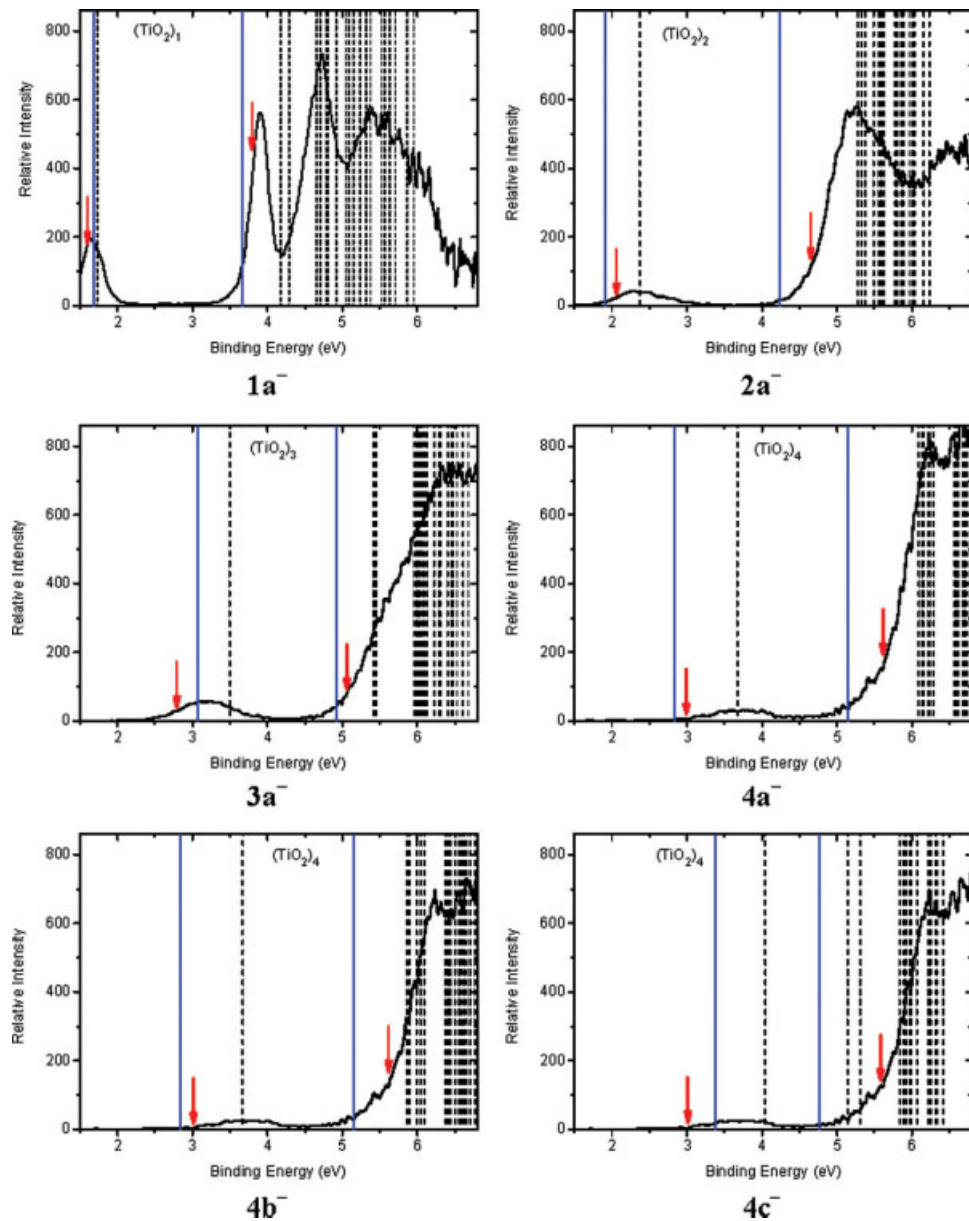


Figure 3. The simulated APES spectra of anionic $(\text{TiO}_2)_n^-$ clusters with cluster size $n = 1-10$. The first and second vertical blue solid sticks indicate the first and second ADE values, respectively, while the vertical black dashed sticks indicate the VDE values. The experimental APES spectra (ref. 10) are shown as black solid curve for comparison. The first and second red arrows indicate the experimentally estimated first and second ADE values, respectively. [Color figure can be viewed in the online issue, which is available at www.interscience.wiley.com]

by the minor contribution from vibrational “hot bands” near the onsets of both X and A bands, by the vibrational broadening of each electron detachment band, and by the congestion of higher electronic states to the A band. These facts make the extraction of accurate ADE and VDE from experimental APES spectra quite difficult. Experimentally, the ADE values were estimated by determining the X and A band onsets, approximately by drawing straight lines along the corresponding leading (lower energy

side) band edges and then adding the instrumental resolution to the intersections with the binding energy axis.¹⁰ As can be seen from Figure 3, the predicted ADE and VDE values for the weak, separated, X band are typically in quite good agreement (mostly within experimental uncertainty of about 0.2 eV)¹⁰ with the experimental data. This could be partially due to the simple electronic origin of the X band, i.e., electron detachment of anionic cluster into the neutral singlet ground state. However, no separa-

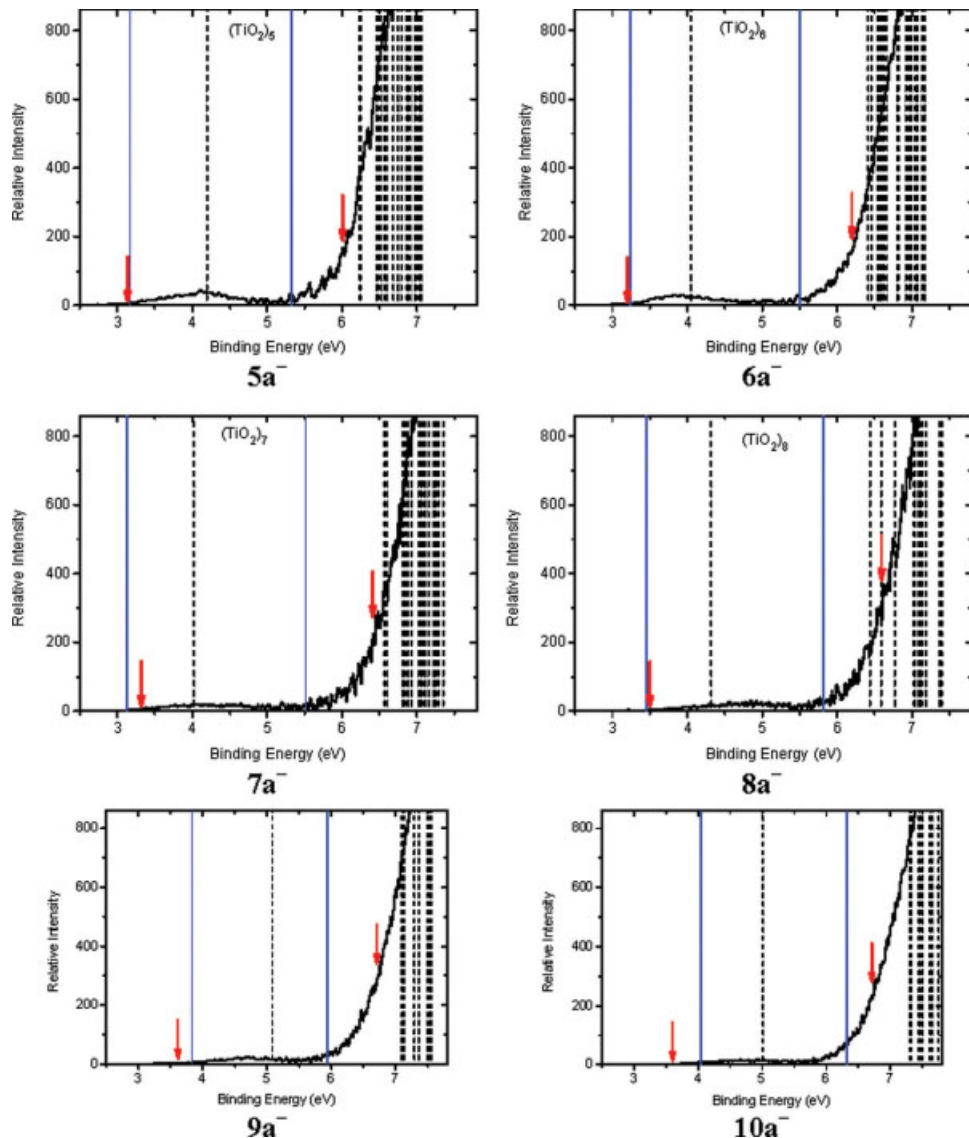


Figure 3. (Continued)

rated A band could be observed in experimental PES spectra except for that of the smallest TiO_2^- cluster.^{9,10} According to our TDDFT results, the experimentally observed “A band” with exceedingly high intensity is actually due to congested triplet and singlet excited states with strong vibrational broadening. Even for the simplest case of TiO_2^- , the intensity of “A band” is about three times as strong as that of X band, mainly due to contributions from near-degenerate triplet and singlet excited states to the former. Thus, the second ADE values estimated¹⁰ by drawing straight line along the leading edge of “A band,” can be evidently overestimated by up to 0.8 eV, especially for larger clusters with $n \geq 5$. As the result, the AGA values are artificially overestimated by the crude experimental analysis.¹⁰ One simple remedy could be suggested according to our theoretical analysis: a straight line along the A band leading edge of each anionic cluster should be drawn from the position with a relative inten-

sity of about 3–4 times as strong as the X band, by assuming that the A band onset is mainly due to the lowest triplet and singlet electronic excited states.

Figure 4 shows the size-dependence of the B3LYP/6-31+G(d) predicted VEA and AEA values for the lowest-lying $(\text{TiO}_2)_n$ clusters and a comparison with the experimental AEA (first ADE) values estimated¹⁰ from APES spectra. The predicted AEA and VEA values tend to increase rapidly with the cluster size n , with the VEA values being very close to AEA values for small clusters but more than 0.8 eV smaller than AEA values for large clusters with $n \geq 4$. The sizable differences between AEA and VEA are consistent with the large structural relaxation after electron attachment as discussed above. Compared with our previous B3LYP/LANL2DZ calculations,¹⁶ the same set of anionic global minima with $n = 2, 3, 6$, and 9 are predicted in this work. However, the B3LYP/LANL2DZ cal-

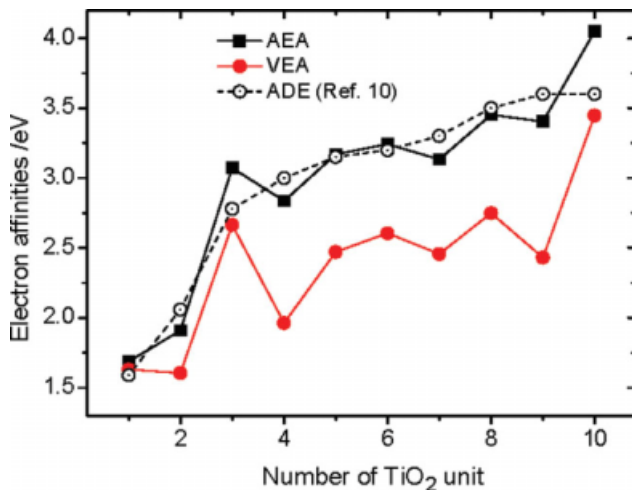


Figure 4. The size-dependence of the B3LYP/6-31+G(d) predicted VEA and AEA (or ADE by definition) values and a comparison with experimentally (ref. 10) estimated ADE values.

culations¹⁶ consistently overestimated the corresponding AEA values by about 0.1–0.5 eV as compared with the experimental^{9,10} and our new B3LYP/6-31+G(d) results, indicating the crucial role of diffusion and polarization functions in 6-31+G(d) basis set for reliable AEA values.

Figure 5 shows the size-dependence of the predicted AGA, VGN, and VGA values and a comparison with the experimentally estimated AGA values.¹⁰ For small $(\text{TiO}_2)_n$ clusters with $n = 1\text{--}4$, all these excitation gaps show strong odd–even oscillation in accordance with our previous DFT results.¹⁶ The predicted AGA values of even- n clusters are almost constant at about 2.3 eV, with those of odd- n clusters being somewhat smaller. In most cases, the predicted VGA values are very close to the corresponding AGA values, which could be due to the partial cancellation of relaxation energies for the first and second ADE values. The experimentally estimated AGA values for small clusters with $n = 1\text{--}4$ are about 0.2 eV larger than our DFT results. For larger clusters the experimentally estimated¹⁰ AGA values increase rapidly to reach the anatase bulk band gap at 3.2 eV, mainly due to the artificially overestimated second ADE values rather than a real “discrepancy” as discussed above. For large neutral clusters with $n \geq 4$, the predicted VGN values may vary around 4.0 eV and are still far above the anatase bulk band gap at 3.2 eV.

In some literature^{9–13} the term “band gap” is used to represent the AGA of metal oxide clusters. However, due to crystal lattice constraint, geometrical relaxation upon bulk optical excitation should be negligible. Thus, it is the VGN of neutral nanoparticles (VGN) that should be directly compared with the experimentally observed optical band gaps of neutral nano-particles and bulks. In other words, the AGA data may be used to represent optical band gap only if the relaxation energy (i.e., the differences between VGN and AGA) upon electronic excitation is negligible. For $(\text{TiO}_2)_n$ clusters with $n \geq 4$, the relaxation energies can be larger than 1.6 eV, leading to the observed surprisingly small AGA.^{9,10} On the other hand, strong structural

relaxation after electron attachment could be expected for most transition metal oxide clusters due to their high EA in general. This means that the VGA values from APES experiment again can not represent accurately the band gaps of neutral metal oxide clusters. It should also be pointed that within the most stable crystal forms of rutile and anatase of TiO_2 , each Ti-atom is six-fold coordinated by O-atoms while each O-atom is threefold coordinated. On the other hand, within the lowest-lying $(\text{TiO}_2)_n$ clusters with n up to 10, most Ti atoms are fourfold coordinated while most O-atoms are twofold coordinated with only small portion being threefold coordinated. In this sense, even the largest $(\text{TiO}_2)_{10}$ cluster is still far from being representative for TiO_2 bulk structure. However, for small TiO_2 nano-crystals of 1–2 nm with high surface-to-bulk ratio, the surface structures with lower-coordinated Ti and O-atoms may contribute significantly to (or even dominate) the observed properties. For example, on the most stable rutile (110) surface there are abundant five-coordinated Ti and two-coordinated O atoms. These facts would make the comparison of electronic properties between our cluster models and bulk TiO_2 to be quite natural to understand the size effect evolution. As further benchmark, B3LYP/6-31+G(d) optimization and TDDFT calculations are performed for the suggested larger $(\text{TiO}_2)_{15}$ defect-free rutile nano-crystal¹⁷ that contains five- and sixfold coordinated Ti-atoms. The predicted VGN and VGA values are 3.759 and 3.001 eV, respectively, with the former being evidently larger than the rutile bulk band gap of about 3.0 eV. Thus, in accordance with the recent experimental¹⁴ and theoretical¹⁷ findings, our predicted VGN values strongly suggest that a clear blue-shift of band gap due to quantum confinement effect can be observed for TiO_2 nano-particles with diameter of about 1 nm.

Conclusions

The electronic structure and stability of both anionic and neutral $(\text{TiO}_2)_n$ ($n = 1\text{--}10$) nano-clusters are investigated by exten-

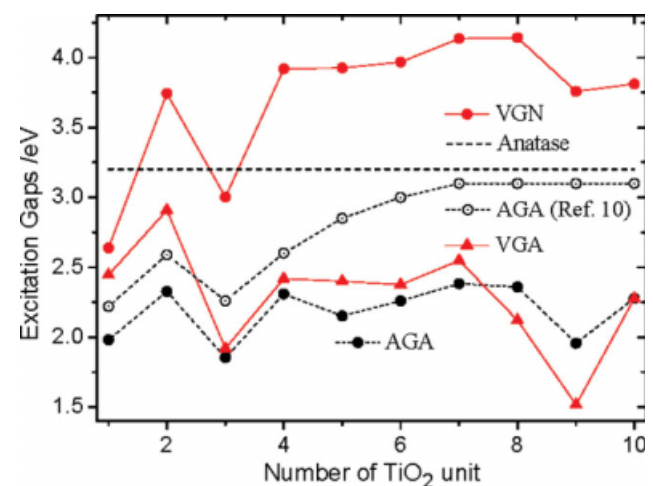


Figure 5. The size-dependence of the B3LYP/6-31+G(d) predicted AGA, VGA, and VGN values and a comparison with experimentally (ref. 10) estimated AGA values. The VGN values should be compared with the bulk anatase band gap of about 3.2 eV.

sive DFT calculations. The main conclusions can be drawn as below: (a) large difference up to 1.5 eV between VDE and VEA values can be observed for large clusters due to strong structural relaxation after electron attachment; (b) the very strong A bands observed in APES experiment are due to multiple rather than single electronic origins; (c) the VGA and AGA values of large anionic cluster are evidently smaller than the VGN of the neutral counterpart, which may also be case for other metal oxide clusters with high EA; (d) the VGN values of neutral $(\text{TiO}_2)_n$ nano-clusters show a clear blue-shift relative to bulk band gap.

Acknowledgments

We thank Dr. Hua-Jin Zhai and Prof. Lai-Sheng Wang for providing us with the experimental APES spectra data. The authors are grateful to Prof. Reinhard Schinke (Max-Planck-Institut für Dynamik und Selbstorganisation, Göttingen) and Mr. Burkhard Bunk (Humboldt Universität zu Berlin, Institut für Physik) for computational facilities.

References

- Rao, C. N. R.; Raveau, B. *Transition Metal Oxides*; Wiley-VCH: New York, 1995.
- Hagfeldt, A.; Gratzel, M. *Chem Rev* 1995, 95, 49.
- Grätzel, M. *Nature* 2001, 414, 338.
- Fernandez-Garcia, M.; Martnez-Arias, A.; Hanson, J. C.; Rodriguez, J. A. *Chem Rev* 2004, 104, 4063.
- Diebold, U. *Surf Sci Rep* 2003, 48, 53.
- Linsebigler, A. L.; Lu, G.; Yates, J. T., Jr. *Chem Rev* 1995, 95, 735.
- Zhang, H.; Banfield, J. F. *J Mater Chem* 1998, 8, 2073.
- Rienstra-Kiracofe, J. C.; Tschumper, G. S.; Schaefer, H. F.; Nandi, S.; Ellison, G. B. *Chem Rev* 2002, 102, 231.
- Wu, H.-B.; Wang, L.-S. *J Chem Phys* 1997, 107, 8221.
- Zhai, H.-J.; Wang, L.-S. *J Am Chem Soc* 2007, 129, 3022.
- Zhai, H.-J.; Li, S.; Dixon, D. A.; Wang L.-S. *J Am Soc Chem* 2008, 130, 5167.
- Zhai, H.-J.; Döbler, J.; Sauer, J.; Wang L.-S. *J Am Soc Chem* 2007, 129, 13270.
- Huang, X.; Zhai, H.-J.; Li, J.; Wang L.-S. *J Phys Chem A* 2006, 110, 85.
- Satoh, N.; Nakashima, T.; Kamikura, K.; Yamamoto, K. *Nature Nanotech* 2008, 3, 106.
- Monticone, S.; Tufeu, R.; Kanaev, A. V.; Scolan, E.; Sanchez, C. *Appl Surf Sci* 2000, 162, 565.
- Qu, Z.-W.; Kroes, G.-J. *J Phys Chem B* 2006, 110, 8998.
- Qu, Z.-W.; Kroes, G.-J. *J Phys Chem C* 2007, 111, 16808.
- Asmis, K. R.; Santambrogio, G.; Brümmer, M.; Sauer, J. *Angew Chem Int Ed* 2005, 44, 3122.
- Huang, X.; Zhai, H.-J.; Li, J.; Wang, L.-S. *J Phys Chem A* 2006, 110, 85.
- Kohn, W.; Sham, L. *J Phys Rev* 1965, 140, A1133.
- Becke, A. D. *J Chem Phys* 1993, 98, 5648.
- Lee, C.; Yang, W.; Parr, R. G. *Phys Rev B* 1988, 37, 785.
- Rassolov, V. A.; Pople, J. A.; Ratner, M. A.; Windus, T. L. *J Chem Phys* 1998, 109, 1223.
- Clark, T.; Chandrasekhar, J.; Spitznagel, G. W.; Schleyer, P. v. R. *J Comp Chem* 1983, 4, 294.
- Frisch, M. J.; Trucks, G. W.; Schlegel, H. B.; Scuseria, G. E.; Robb, M. A.; Cheeseman, J. R.; Montgomery, J. A., Jr.; Vreven, T.; Kudin, K. N.; Burant, J. C.; Millam, J. M.; Iyengar, S. S.; Tomasi, J.; Barone, V.; Mennucci, B.; Cossi, M.; Scalmani, G.; Rega, N.; Petersson, G. A.; Nakatsuji, H.; Hada, M.; Ehara, M.; Toyota, K.; Fukuda, R.; Hasegawa, J.; Ishida, M.; Nakajima, T.; Honda, Y.; Kitao, O.; Nakai, H.; Klene, M.; Li, X.; Knox, J. E.; Hratchian, H. P.; Cross, J. B.; Bakken, V.; Adamo, C.; Jaramillo, J.; Gomperts, R.; Stratmann, R. E.; Yazyev, O.; Austin, A. J.; Cammi, R.; Pomelli, C.; Ochterski, J. W.; Ayala, P. Y.; Morokuma, K.; Voth, G. A.; Salvador, P.; Dannenberg, J. J.; Zakrzewski, V. G.; Dapprich, S.; Daniels, A. D.; Strain, M. C.; Farkas, O.; Malick, D. K.; Rabuck, A. D.; Raghavachari, K.; Foresman, J. B.; Ortiz, J. V.; Cui, Q.; Baboul, A. G.; Clifford, S.; Cioslowski, J.; Stefanov, B. B.; Liu, G.; Liashenko, A.; Piskorz, P.; Komaromi, I.; Martin, R. L.; Fox, D. J.; Keith, T.; Al-Laham, M. A.; Peng, C. Y.; Nanayakkara, A.; Challacombe, M.; Gill, P. M. W.; Johnson, B.; Chen, W.; Wong, M. W.; Gonzalez, C.; Pople J. A. Gaussian 03, revision D. 01; Gaussian, Inc.: Wallingford, CT, 2004.
- Hamad, S.; Catlow, C. R. A.; Woodley, S. M.; Lago, S.; Mejias, J. A. *J Phys Chem B* 2005, 109, 15741.
- Calatayud, M.; Maldonado, L.; Minot, C. *J Phys Chem C* 2008, 112, 16087.
- Stratmann, R. E.; Scuseria, G. E.; Frisch, M. J. *J Chem Phys* 1998, 109, 8218.
- Bauernschmitt, R.; Ahlrichs, R. *Chem Phys Lett* 1996, 256, 454.
- Casida, M. E.; Jamorski, C.; Casida, K. C.; Salahub, D. R. *J Chem Phys* 1998, 108, 4439.
- Santambrogio, G.; Brümmer, M.; Wöser, L.; Döber, J.; Sierka, M.; Sauer, J.; Meijer, G.; Asmis, K. R. *PCCP* 2008, 10, 3992.
- Lundqvist, M. J.; Nilsing, M.; Persson, P.; Lunell, S. *Int J Quantum Chem* 2006, 106, 3214.